PERGAMON

Journal of Structural Geology 25 (2003) 1229–1240

JOURNAL OF STRUCTURAL GEOLOGY

www.elsevier.com/locate/jsg

Experimental investigation of shear band patterns in granular material

Henning Wolf*, Diethard König, Theodoros Triantafyllidis

Institute for Soil Mechanics and Foundation Engineering, Ruhr-University Bochum, 44801 Bochum, Germany

Received 12 January 2002; received in revised form 8 October 2002; accepted 11 October 2002

Abstract

This paper presents three series of sandbox experiments of extensional deformation in granular material. The dependence of the developing shear band system on different boundary conditions and material properties is investigated: (1) granulometric properties of the material, (2) initial geometry of the specimen, and (3) dynamic material parameters. Particular attention is paid to the controlling of the basal boundary conditions. X-ray technique and particle image velocimetry (PIV) are used to study the changes in the granular structure and in the formation of shear band patterns. The results show that boundary conditions are an elaborate factor to explain differences in the shear band pattern. It is shown that neither the average grain size diameter d_{50} nor the rate of loading influences the shear band spacing. The spacing of the bands seems to be linearly dependent on the initial height of the specimen.

Keywords: Extension; Sandbox experiments; Shear band patterns; X-ray technique

1. Introduction

Sandbox experiments can be used to study the development of shear band patterns in different granular materials under variation of boundary conditions such as initial height or width of the specimen. Patterns of shear bands in soils or granular materials can be identified in relevant laboratory models, in the scale of earth retaining structures as well as in geological formations. These patterns are important for the stress–strain behaviour of the materials consisting of soil or rock and for the analysis of soil–structure interaction problems. The factors governing the process of shear banding in granular materials are not clarified yet. It remains unknown to what extent the geometry of patterns of shear bands depends on the boundary conditions of the selected system and/or on the properties of the material under investigation.

The appearance of shear banding is well documented in several papers in the field of civil engineering as well as in the field of geology. In soil mechanics, the phenomenon of initiation and propagation of shear bands has been investigated theoretically and experimentally by a great number of researchers (Coulomb, 1773; Roscoe, 1970; Vardoulakis, 1980; Vardoulakis and Goldscheider, 1980; Desrues et al., 1985; Mühlhaus and Vardoulakis, 1987; Tatsuoka et al., 1990; Vermeer, 1990; Han and Drescher, 1993; Papamichos and Vardoulakis, 1995; Finno et al., 1997; Yoshida and Tatsuoka, 1997; Mokni and Desrues, 1998; Oda and Kazama, 1998; Saada et al., 1999; Alshibli and Sture, 2000). All mentioned researchers concentrate their efforts on examining the factors governing the behaviour of a single shear band; descriptions of systems of shear bands are rare.

Vermeer (1990) summarised results of direct shear tests and biaxial tests (Arthur et al., 1977; Arthur and Dunstan, 1982; Duthilleul, 1982; Desrues, 1984) with respect to the dependence of the inclination of shear bands on particle sizes of sand. He pointed out that Coulomb-type shear bands, with the angle of inclination θ_C, appear in experiments with fine sand and Roscoe-type shear bands, with the angle of inclination θ_R, develop in experiments with coarse sand.

Eq. (1) specifies the orientation of a shear band against the direction of minor compressive stress as defined by Coulomb (1773):

$$\theta_C = 45° + \phi/2 \tag{1}$$

where ϕ represents the internal friction angle of the material. Eq. (1) satisfies the Mohr–Coulomb hypothesis that the direction of a shear band coincides with the direction of the plane, where the ratio of shear stress and normal stress reaches a maximum. Eq. (2) shows the

* Corresponding author.
E-mail address: hw@gub.ruhr-uni-bochum.de (H. Wolf).

0191-8141/03/$ - see front matter © 2002 Elsevier Science Ltd. All rights reserved.
PII: S0191-8141(02)00163-3

orientation of a shear band against the direction of minor compressive stress as defined by Roscoe (1970):

$$\theta_R = 45° + \nu/2 \quad (2)$$

where ν denotes the angle of dilatancy. Roscoe's theory is based on the use of a plastic flow rule in combination with the assumption of coaxiality of principle stress rate and plastic strain rate.

Bransby and Milligan (1975) investigated the deformation behaviour of dense and loose soil behind fixed retaining walls. By using X-rays they observed systems of shear bands, inclined to the vertical by the angle of Roscoe θ_R (1970). Their research deals with the inclination of the rupture surfaces, statements concerning the spacing cannot be found. On the basis of the Bransby and Milligan data set, Lesnièwska and Mróz (2000, 2001) developed an analytical solution of the phenomenon of shear banding behind retaining walls. In their theoretical concept, softening of the soil is included, i.e. the decreasing of the internal friction angle ϕ_0 at the peak to the critical state friction angle ϕ_{crit} with increasing strain. They calculate distances of shear bands in good agreement with the distances obtained from X-ray pictures.

Further examples of shear banding can be found in the research on numerical simulation of shear band patterns as done by Mühlhaus and Aifantis (1989), Tejchman and Wu (1993) or Nübel and Karcher (1999). Poliakov et al. (1994) investigated the dependence of shear band formation on dynamic soil parameters. They simulated systems of shear bands numerically by the finite difference method, applying pure shear on a square sample of an elasto-plastic medium. In addition to the loading velocity v_{bc} at the boundaries of the sample, the confining pressure p and the material constants (cohesion c, internal friction angle ϕ and angle of dilatancy ν), dynamic soil parameters (shear modulus G_{dyn} and the p-wave velocity v_p) had been varied to study their influence on the shape of the shear band systems. As the strain increases it can be observed that shear bands form spontaneously in regions in which plastic deformation occurs. These bands show an angle of inclination θ with respect to the horizontal of $45° - \phi/2 < \theta < 45° - \nu/2$.

Poliakov et al. (1994) pointed out that the thickness of the single shear bands is not related directly to the material constants ϕ and ν but to the difference between them. A small difference in angle gives thick and regular shear bands, whereas a larger difference leads to thinner and more irregular bands. On the other hand the failure angle of the shear bands is directly dependent on the material parameters ϕ and ν.

Poliakov et al. (1994) introduced a nondimensional parameter B, defined as follows:

$$B = \frac{\sigma v_p}{G_{dyn} v_{bc}} \quad (3)$$

where σ denotes the confining pressure, G_{dyn} represents the dynamic shear modulus, and v_p/v_{bc} is the ratio of the p-wave velocity and the velocity of loading. They developed a hypothesis that the factor B controls the behaviour of the shear band system. In particular,

(a) changing the various parameters does not affect the results as long as B is kept unchanged: both the evolution and the spacing of the shear bands depend only on this parameter,
(b) an increase in B leads to an increase in shear band spacing and vice versa.

The latter is explained by Poliakov et al. (1994) as follows: when a shear band forms, this process is accompanied by a decrease in stress inside and an increase in stress outside the band. This increase in stress inhibits the formation of a new shear band adjacent to the former one. The stress difference propagates through the material with p-wave velocity. Hence a large value of B, synonymous with a large p-wave velocity, leads to widely separated shear bands.

Using the finite-difference code FLAC, Harper et al. (2001) investigated the influence of the type of basement extension on faulting in cover sediments. They simulated uniformly or non-uniformly extended sand packages whereupon non-uniform extension is induced by modelling a stick-slip behaviour of the extending basement. The sand is given various material properties (e.g. homogeneous sand, sand with heterogeneous mechanical properties, sand with an initial density heterogeneity and strain-softening sand). Harper et al. (2001) concluded that no significant shear bands develop for uniform basement extension and homogeneous sand, unless the sand has strain-softening properties. Because shear bands developed weakly even with strongly strain softening sand, Harper et al. (2001) suggested that the rubber membrane in the sandbox experiments performed by McClay and Ellis (1987a,b) and Vendeville et al. (1987) did not extend uniformly.

In addition to the mentioned sandbox experiments, other tests have been performed by geologists using analogue models to simulate tectonic faulting or in other words systems of shear bands (Mandl, 1988; McClay, 1989, 1990). In all experiments the ductile lower crust of the earth was simulated by the use of a rubber membrane, whereas the brittle crust was modelled by a layer of granular material as e.g. sand. McClay and Ellis (1987a,b) and McClay (1990) performed sandbox experiments and investigated fault initiation, fault propagation, and rotation of shear band systems, as well as the geometric evolution of individual fault planes. McClay (1989) investigated extension followed by contraction of the same specimen. In sandbox experiments Vendeville et al. (1987) focused on fault location and fault spacing. They concluded that the spacing between single shear bands inside a system of fault planes is a measure of the thickness of the layer.

Gapais et al. (1991) presented results of plane–strain sandbox experiments on dry quartz sand. They imposed different kinematic conditions (e.g. simple shear) and

observed initial fault orientations in accordance with the Coulomb criterion. They concluded that strong similarities exist between the generated fault systems and other shear zone patterns due to simple kinematic factors.

In conclusion, the appearance of shear band systems in several examples in the fields of civil engineering and geology is dependent on boundary conditions and material parameters. The aim of this paper is to study the influence of these parameters on the shape of shear band systems, described by the spacing between bands, their inclination and the evolution of the fault planes. Although modelling the ductile lower crust with a rubber membrane is not representative of real conditions, sandbox experiments are a useful tool to investigate those dependencies.

In the following we present the investigation of shear band patterns in different material or soil samples under variation of the following material parameters and boundary conditions: (1) granulometric parameters (average grain size d_{50} and coefficient of uniformity $U = d_{60}/d_{10}$), (2) geometry of the sample, and (3) dynamic material properties as defined by Poliakov et al. (1994). Particular attention is paid to the method of measuring distances and inclinations inside the specimens and to the homogeneity of basal boundary conditions.

2. Experimental method and testing program

2.1. Model set-up

According to the various experiments of McClay an experimental device (Fig. 1) was constructed. The specimen lies on a thin rubber membrane and is surrounded by plexiglass-walls. The rubber membrane, which applies the strain to the specimen, is fixed at one side and fastened to a movable wall at the other side. Furthermore the construction of the model set-up is suited to special requirements as described in the following.

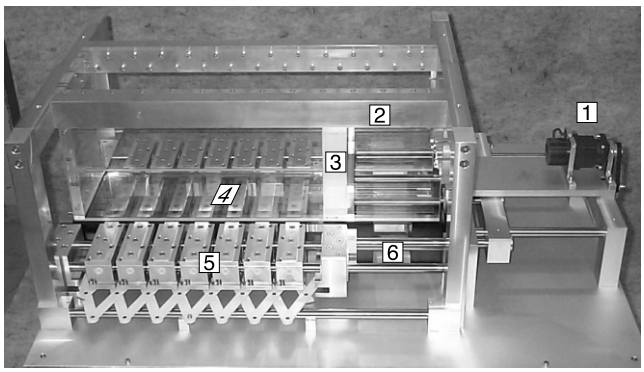

Fig. 1. Experimental device: (1) motor, (2) frame with plexiglass walls surrounding the specimen, (3) movable wall, (4) horizontal base plate made of glass, (5) metal bars with scissor mechanism, (6) system of rods to move the bars and the movable wall. The rubber sheet (not shown here) is placed on the base plate and is fixed at the movable wall, at the steel bars and at the end of the device (on the left in the picture).

With reference to the Harper et al. (2001) inference that the basement in the numerous experiments of McClay, Ellis and Vendeville (see previous references) did not extend uniformly and with respect to a good reproducibility of the results, we paid particular attention to the requirement that the device should provide a constant distribution of strains in the rubber membrane and thus a constant strain distribution in the specimen. The rubber sheet is linked with a combination of metal bars that slide on ball bearings and parallel steel rods. The bars are connected by a mechanism of scissors. During stretching of the rubber, the scissor mechanism ensures that the distance between the bars is kept constant at any rate of displacement and thus the strain distribution in the rubber sheet remains homogeneous. The distribution of the strain in the rubber can be controlled by surveying a mesh on the bottom side of the membrane through the base plate.

An additional requirement that has to be taken into account is the optimal dimension of the width of the specimen. On the one hand the sample should be as wide as possible in order to reduce the influence of friction between the sample and the side walls. On the other hand the width should be as small as possible in order to ensure the feasibility of taking X-ray pictures of the interior of the specimen with the available X-ray apparatus. Several tests have been performed in advance resulting in an optimal width of the specimen of 20 cm. The influence of the side wall friction has been minimized by using polished plexiglass as sidewall material. Observations of the surface of the specimen show that the shape of the shear bands over the width of the specimens is almost straight with just small curvatures in the contact area of shear bands and side walls.

The maximum length of the specimen is 70 cm in final extension state, the minimum length in initial state is 50 cm, thus a displacement of 20 cm can be imposed. The maximum height of the sample is 30 cm. In order to investigate at a later date the influence of the stress level and the stress gradient on the spacing of the shear bands, the whole device is designed for use in the 'Bochum Geotechnical Centrifuge' to stand an increased gravity-level of at least 30 times the earth acceleration.

2.2. Observation of the model

Particular attention is paid to the method of measuring distances and inclinations inside the specimens. The disadvantage of many former investigations, not knowing which processes take place inside the sample and using measurement techniques that do not allow the identification of shear bands before reaching large deformations, is eliminated by using a mobile C-arm X-ray system. X-ray technique is able to portray differences in density of the granular material and thus to offer the opportunity to record changes in the granular structure inside the specimen (e.g. Bransby and Milligan, 1975). The X-ray apparatus we used enables a continuous observation and recording of the

processes inside the sample. Thus the point of time and the value of strain when the first shear bands appear can be determined exactly. Single pictures of the movie taken with the X-ray apparatus are evaluated with a computer program. The determination of the shear band spacing is within a precision of 0.1 mm.

To make propositions concerning the strain distribution in and between the shear bands, digital pictures of the sides of the specimen are taken and evaluated with an image analysis technique, called 'particle image velocimetry (PIV)'. In comparison with well-known examples of image processing, such as e.g. laser speckle technique (Tatsuoka et al., 1990), computed tomography (Desrues et al., 1996) and stereophotogrammetry (Desrues et al., 1985; Viggiani et al., 2001), the PIV-method calculates the displacement field of the grains at the side of the specimen and hence the strains and rotations in the granular structure. The measurable displacements of the grains can be very small, depending on the size of the pictures and the resolution of the digital camera. Combining the camera resolution of 1 megapixel with the size of the pictures, we receive a theoretical displacement accuracy of 0.125 mm/pixel. The PIV-method enables us to identify the position and the inclination of the shear bands at a very early stage of the experiment, whereas no changing in the structure can be observed on the sides by eye. If the stretching of the rubber membrane is continued, shear bands can be detected by a coherent skip in lines of coloured material, which have been included in certain steps during the preparation of the specimen.

2.3. Construction of the model and model deformation

As detected by several researchers (Mandl et al., 1977; Krantz, 1991; Schellart, 2000; Cobbold et al., 2001) the density of the prepared specimen, and thus the mechanical properties of the material, is heavily dependent on the preparing method of the sample and on the composition of the material. In our experiments the material is poured by the raining method with the help of a hopper and a sieve keeping a constant distance of 30 cm from the actual surface of the specimen. Using this method, we obtain a homogeneous density inside the specimen of $D = 1.0$. Layers of coloured material are included in certain steps. After finishing the model construction the movable wall and the scissor mechanism are displaced in order to apply homogenous strain to the specimen. Even if the X-ray apparatus is able to record continuously the density changes inside the specimen, it is not possible to take X-ray shots of all regions of the sample simultaneously. In order to provide a sufficient amount of data to calculate the distances and inclinations, the process of moving the wall and thus applying strain into the specimen is stopped at well-defined stages of the experiment to take radiographs of all regions of the sample. During the first centimetres of stretching, the sides are recorded with a digital video camera. Pictures for the evaluation with the PIV-method can be exported from this film.

2.4. Materials

We used quartz sand (Siligran®), artificial particles (urea resin), chilled iron grit and glass beads in our experiments. Except for the quartz sand, all materials have been obtained from a commercial supplier of blasting systems and blast media. A list of all material parameters is presented in Table 1. All parameters have been determined in the laboratory of the Institute for Soil Mechanics and Foundation Engineering of the Ruhr-University of Bochum by performing triaxial tests and standard laboratory tests, such as determination of the grain size distribution or the determination of the grain density. The dynamic shear modulus G_{dyn} has been measured by performing tests in the resonant-column apparatus, which is an apparatus to measure directly the dynamic properties (e.g. shear wave velocity v_s, dynamic shear modulus G_{dyn} and material damping) of a column consisting of granular material at resonant frequencies of the system (Wichtmann et al., 2001).

2.5. Testing programme

Three test series have been performed (Tables 2–4). In the first series (Table 2), the influence of the granulometric

Table 1
Material parameters

No.	Material	Grain shape (–)	d (mm)	d_{50} (mm)	U (–)	ϕ (°)	ν (°)	γ(D = 1.0) (kN/m^3)	ρ_s (g/cm^3)	G_{dyn} (N/mm^2)	v_p (m/s)	θ_C (°)	θ_R (°)
1a	Quartz sand	Equidimensional	0.1–0.71	0.35	1.5	45.0	15.0	17.30	2.64	178	590	67.5	52.5
1b	Quartz sand	Equidimensional	1.0–2.0	1.58	1.5	47.0	20.0	16.05	2.64	–	–	68.5	55.0
1c	Quartz sand	Equidimensional	0.06–2.0	0.85	5.1	44.5	16.5	18.30	2.64	–	–	67.3	53.3
1d	Quartz sand	Equidimensional	0.5–1.2	0.89	1.5	45.0	–	16.40	2.64	–	–	67.5	–
2	Artificial particles	Equidimensional	0.1–0.4	0.35	1.5	37.0	8.0	7.95	1.55	32	395	63.5	49.0
3	Glass beads	Round	0.06–1.0	0.32	1.4	33.0	12.0	15.90	2.50	170	618	61.5	51.0
4	Iron grit	Equidimensional	0.06–0.5	0.24	1.7	47.0	13.5	37.30	7.27	95	288	68.5	51.8

Notes: d: grain diameter; d_{50}: average grain diameter; U: coefficient of uniformity; ϕ: friction angle at the peak; ν: angle of dilatancy; ρ_s: density of the grains; G_{dyn}: dynamic shear modulus; v_p: p-wave velocity; θ_C: shear band inclination (Coulomb); θ_R: shear band inclination (Roscoe); γ: unit weight.

Table 2
Test series 1: granulometric parameters

Experiment	Material	Average grain diameter (d_{50}) (mm)	Grain diameter (d) (mm)	Coefficient of uniformity (U) (–)
SFA02/SFA03	1a	0.35	0.1–0.71	1.5
SFA04/SFA05	1b	1.58	1.0–2.0	1.5
SFA06/SFA07	1c	0.85	0.06–2.0	5.1
SFA19/SFA20	1d	0.89	0.5–1.2	1.5

properties of quartz sand on the development of shear band systems has been investigated by changing the coefficient of uniformity U and the range of the grain size distribution. The second series (Table 3) includes the changing of the initial geometry of the specimen by changing the initial height h_0. In the third series (Table 4) we have focused on the dependence of shear band patterns on the dynamic material parameters. In each test, the movable wall has been moved by 20 cm, corresponding to a bulk strain of 40%.

3. Experimental results

3.1. Definition of spacing and inclination

Fig. 2 shows a simplified radiograph of an arbitrarily chosen part of experiment SFA03, for a strain of 10%. The bright regions represent shear bands that have formed as a result of strain loading. Corresponding to Fig. 2, the shear band spacing a is defined as the distance between the middle axes of two adjacent shear bands, d_{SB} as the thickness of the shear band, b as the width of the block between two flanking shear bands, and θ as the inclination of the shear bands with respect to the horizontal.

3.2. Initiation and evolution of shear band systems

The first changes in the granular structure of the investigated specimen can be observed in all experiments nearby the fixed and the movable wall after small amounts of applied strain ($\approx 1\%$). The forming shear bands are inclined between $\theta_C = 45° + \phi/2$ and $\theta_R = 45° + \nu/2$ to the horizontal and therefore between the characteristic inclinations determined by the static requirement of Coulomb (1773) and the kinematic requirements of Roscoe (1970), cf. Section 1. Subsequently, a system of shear bands develops abruptly with uniformly distributed shear bands over the entire length of the sample. These shear bands cannot be identified at the sides of the specimen by eye at this early stage of the tests because displacements are not large enough to create offsets in the lines of coloured material. In contrast to this, the pattern of shear bands can be determined on the radiographs as well as on contour plots, evaluated with the PIV-method.

The value of strain when the first shear band patterns appear, subsequently to the development of the shear bands nearby the fixed and movable wall, seems to be dependent on the kind of material investigated. Whereas in the experiments with sand, the first shear bands are detected at a horizontal displacement of the movable wall of 3 cm, which is in accordance with a homogenous strain in the rubber membrane of 6%, the shear bands already develop in the experiments with artificial material and glass beads at a displacement of the moving wall of 1 cm ($\cong$ 2% strain) and 2 cm ($\cong$ 4% strain), respectively.

Nearby the movable wall a horst develops and the orientation of shear bands changes. As no other horst appears along the specimen, the shear bands are inclined in the same direction over the full length of the sample (Fig. 3). In contrast to this observation it was expected that the shear bands appear in conjugated pairs, i.e. they make the same angle to either side of the vertical. As we found out the condition whether conjugated pairs develop or not seems to be dependent on the average grain size of the particles (cf. Section 4).

Table 3
Test series 2: initial geometry of the specimen

Experiment	Material	Initial length (L) (mm)	Width (B) (mm)	Initial Height (H) (mm)
SFA02/SFA03	1a	500	200	150
SFA09/SFA10	1a	500	200	100
SFA16/SFA17	1a	500	200	200

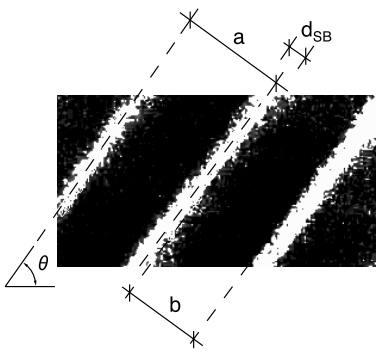

Fig. 2. Definition of distance a as the distance between two adjacent shear bands, d_{SB} as the thickness of the shear band, b as the width of the block between two flanking shear bands and θ as the inclination of the shear bands with respect to the horizontal.

Table 4
Test series 3: variation of the dynamic parameters

Experiment	Material	Factor (B) (–)	Loading velocity (v_{bc}) (cm/min)	Material
SFA02/SFA03	1a	90	0.28670	Quartz sand
SFA22/SFA26	1a	9	2.86700	Quartz sand
SFA23/SFA27	1a	900	0.02867	Quartz sand
SFA08/SFA21	2	90	0.49070	Artificial particles (urea resin)
SFA15/SFA18	3	90	0.28840	Glass beads
SFA25	4	90	0.56570	Iron grit

The following development inside the specimens can be generalized for all experiments and all materials:

1. Shear bands that form in the early stages of the test remain active and plane, even at high strains. No additional shear zone appears. Supplementary strain is accumulated predominantly in the existing localisation zones.
2. Just a small part of the applied strain is gathered in the blocks between the shear bands. This fact is demonstrated by the contour plot of the shear strain, evaluated with the PIV-method with two pictures of the sides of test SFA22 at an imposed strain of 15% (Fig. 4). Furthermore, if we measure the width b of the blocks between the shear bands, we come to the conclusion that the increase of b with stretching of the rubber sheet is much smaller than the increase of the shear band distance a.
3. The thickness d_{SB} of the early formed shear bands in the initial state varies between 6 and 13 times the average grain diameter and increases with rising strain. The inclination of the shear bands decreases linearly with increasing strain. The blocks between the bands rotate in the direction of the moving wall.

The general development of the shape of the shear band systems with increasing strain in experiment SFA03 is exemplarily shown in Fig. 5.

3.3. The influence of different material parameters on the shear band spacing and the shear band inclination

3.3.1. The influence of granulometric parameters

Fig. 6 illustrates results of sandbox experiments respective to the variation of the average grain size diameter d_{50} and the coefficient of uniformity U. It demonstrates that the shear band distance a increases slightly and the shear band inclination θ decreases linearly with increasing strain. By analysing the diagram one might come to the conclusion that the use of coarser material while keeping the coefficient of uniformity constant leads to greater distances between zones of localisation. As we will later see this conclusion is misleading.

The initial shear bands are inclined with an average angle of $\theta = 62°$ to the horizontal. With respect to the material parameters as given in Table 1 and the theories of Coulomb (1773) and Roscoe (1970), observations of Vermeer (1990) are confirmed, whereupon shear bands in fine material are inclined to the horizontal with the angle of Coulomb (θ_C), whereas rupture zones in coarse material correspond to the Roscoe angle (θ_R).

Furthermore, by comparing the results of the experiments in which a sand with a higher coefficient of uniformity was used (SFA06/SFA07) with the results of the other experiments, one can see clearly that the distance a, as well as the inclination θ, corresponds to the test with sand possessing a smaller coefficient of uniformity but the

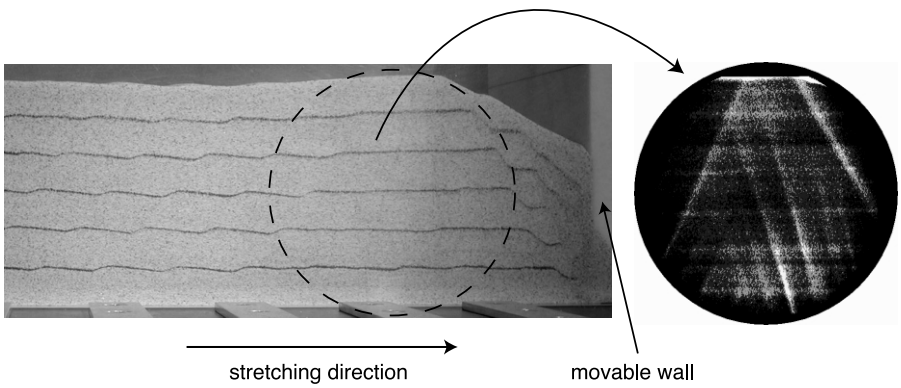

Fig. 3. Change of shear band inclination close to the movable wall (side view and X-ray picture).

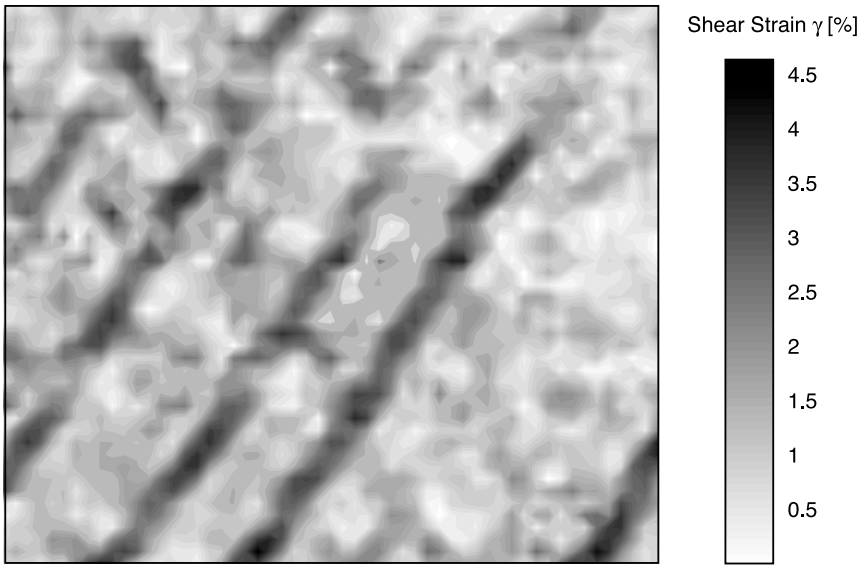

Fig. 4. Contour plot of shear strain (test SFA22) evaluated with the PIV-technique (cf. Section 2.2). The picture has been derived from the middle part of the specimen. Width and height of the picture are 12.5 and 11.0 cm, respectively.

same maximum grain diameter (materials 1b and 1c in Table 1). This shows that the mechanical behaviour and the material parameters related to the maximum grain size govern the shape of the shear bands.

3.3.2. The influence of the initial state geometry

The influence of the variation of the initial height h_0 of the specimen on the distances and the inclinations of the shear bands is summarised in Fig. 7. The diagram shows the shear band distance a and the inclination θ versus the strain ϵ. The clear and nearly linear relationship between the shear band spacing and the initial height of the specimen at a given state of strain is evident.

The inclination of the shear zones does not depend on the initial height of the specimen. This was expected, because the known theories relate the shear band orientation only to mechanical properties of the material (i.e. internal friction angle ϕ and the angle of dilatancy ν), not to boundary conditions. The average angle $\theta = 62°$ at the point when the bands form lies between the values of θ_R and θ_C and confirms again the observations of Vermeer (1990) as mentioned above.

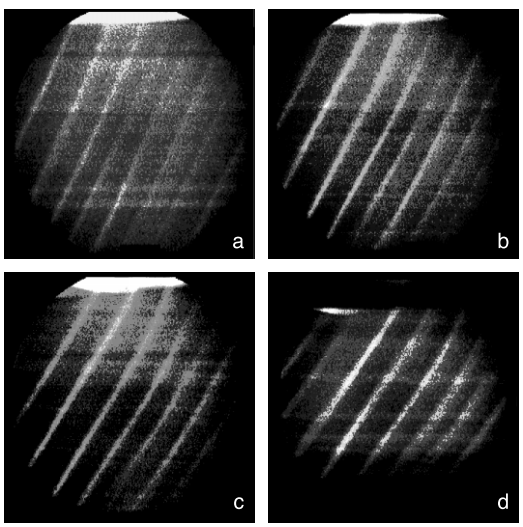

Fig. 5. X-ray pictures of four stages in the development of the shear band system with increasing strain (test SFA03): (a) $\epsilon = 10\%$, (b) $\epsilon = 15\%$, (c) $\epsilon = 20\%$, (d) $\epsilon = 25\%$.

3.3.3. The influence of dynamic parameters

The influence of changing the factor B (Eq. (3)) by varying the loading velocity on the shear banding is presented in Fig. 8. Independent of the value of B, all distances and inclinations coincide at particular stages of the different experiments. Hence, the shapes of the shear band systems are independent of the rate of loading.

Once more the inclination decreases linearly with increasing strain. The average initial angle θ has a value of 62.5° and thus is closer to the angle of Coulomb θ_C than to the angle of Roscoe θ_R.

In Fig. 9, the results of the experiments with constant factor B but varying dynamic parameters are summarized. The inclinations of the shear bands decrease while the distances between the shear bands increase slightly with imposed strain ϵ. In contradiction to Poliakov et al. (1994), the values for the spacing and the inclinations do not coincide.

4. Discussion and interpretation of the experimental results

As mentioned in the introduction, many sandbox experiments have been performed by different researchers. The methods for monitoring the changes in the granular

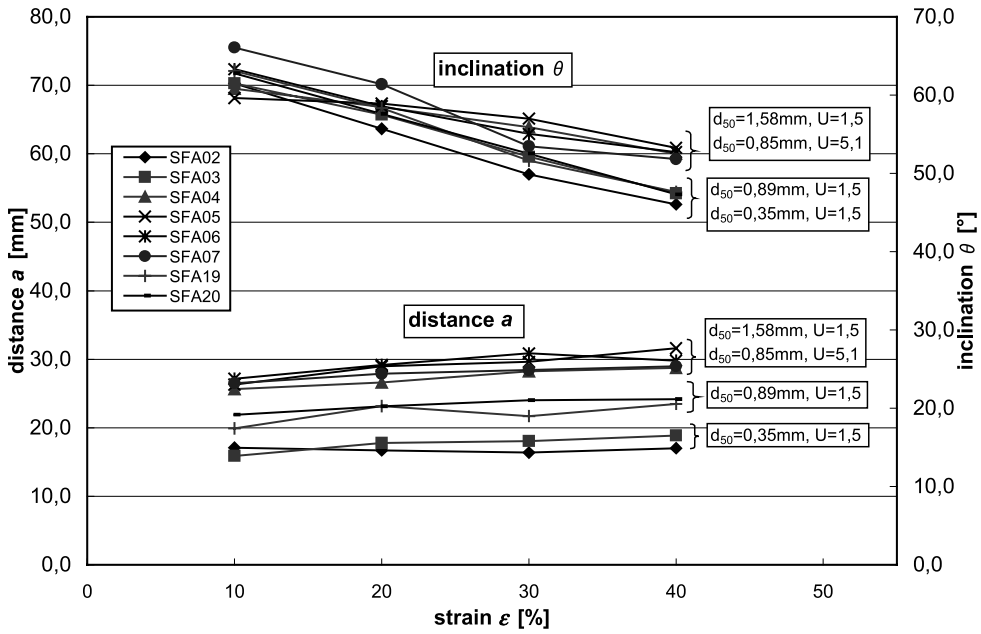

Fig. 6. Influence of granulometric properties on the shear band spacing and the inclination.

structure of the specimens were limited to the evaluation of changes on the visible sides of the sample. From this follows the stringent inference that the results on the sides are transferable to the inner part of the specimen. As we found out, this interpretation is misleading due to the fact that the number of shear bands on the sides cannot be considered as representative for the number of localisation zones inside the specimen. From the evaluation of the X-ray pictures that we took during the tests, it follows that the entire shear band system develops at an early point of the experiments and that even at high strains no additional shear bands occur. On the sides of the specimen only 'strong' and thick shear bands become visible. In addition to the latter, thin but nevertheless active shear zones can only be identified on the radiographs. This observation is in contrast to studies of other researchers (e.g. Ishikawa and Otsuki, 1995) who determine a rising number of fault zones with increasing strain and questions the usefulness of 'fault sequence diagrams' as published by different authors (McClay and Ellis, 1987a,b; McClay, 1989). In addition, the strain dependent development of the initial faults does not fit the assumption of uniformly stretching basement and thus confirms speculations of Harper et al. (2001) who doubt the uniformity of strains in the cited papers. Indeed, the inference of Harper et al. (2001) has to be handled with care because it is not confirmed whether McClay and Ellis

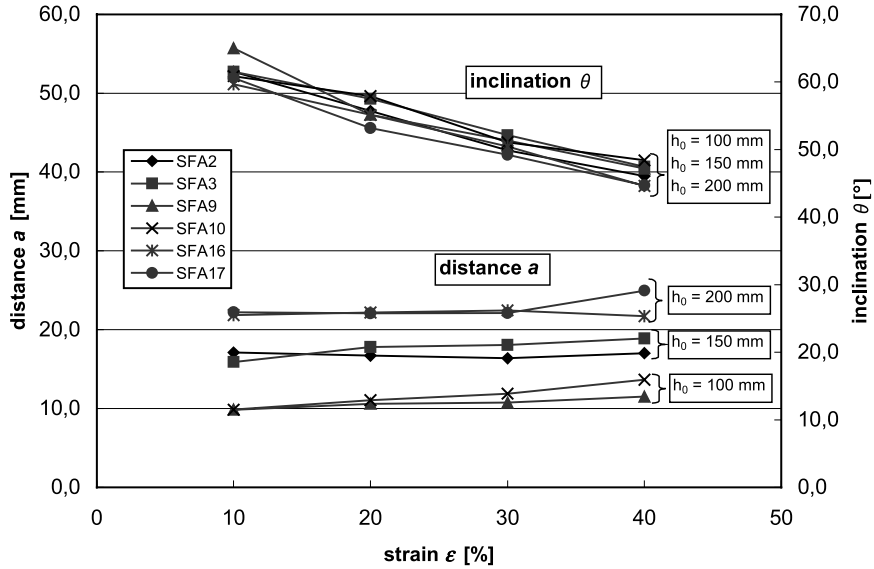

Fig. 7. Influence of the initial geometry of the specimen on the shear band spacing and the inclination.

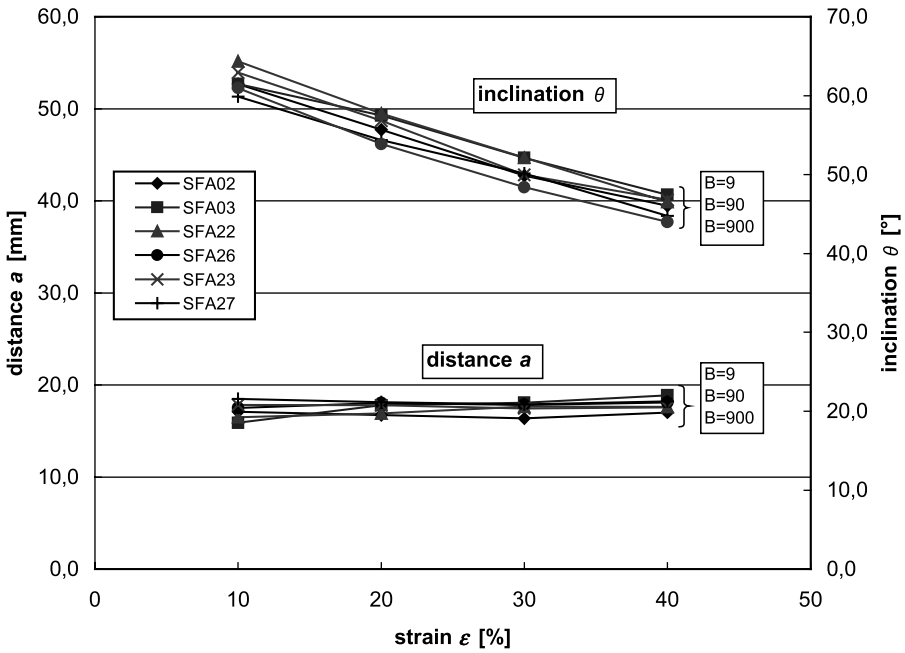

Fig. 8. Influence of varying factor B (Eq. (3)) on the shear band spacing and the inclination.

(1987a,b) and Vendeville et al. (1987) used loose soil or a sand with soil-softening properties or not.

The phenomenon of extensional block rotation is well known in geology and numerously investigated by many researchers such as Mandl (1988), Vendeville and Cobbold (1988), Wernicke and Burchfiel (1982) or Brun et al. (1994). Our experiments confirm these investigations: the inclination of the shear bands decreases linearly between the Coulomb and the Roscoe angle with increasing strain and the fault planes stay planar. The width b between two flanking shear zones remains almost constant (Fig. 10), the blocks rotate in the direction of the moving wall. Thus the deformation within a single fault domain is simple shear.

A requirement for the existence of block rotation is the uniformity of the dip direction of the single shear bands. As we described in Section 3.2, we observed the existence of a horst near the moving wall and a change in the shear band dip direction behind this horst. Mandl (1988, 2000) gives an explanation for this observation that no conjugate shear band system develops but shear bands that are aligned in only one direction. He argues that the occurrence of horizontal shear strains in consequence of the stretching of the rubber membrane disturbs the symmetry of maximum strain and

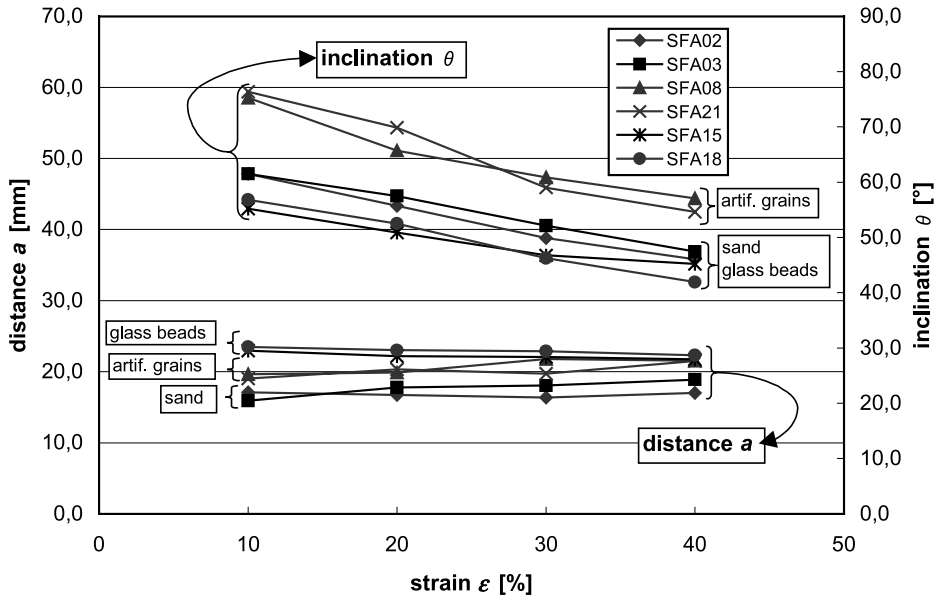

Fig. 9. Influence of constant factor B (Eq. (3)) with varying dynamic parameters on the shear band spacing and the inclination.

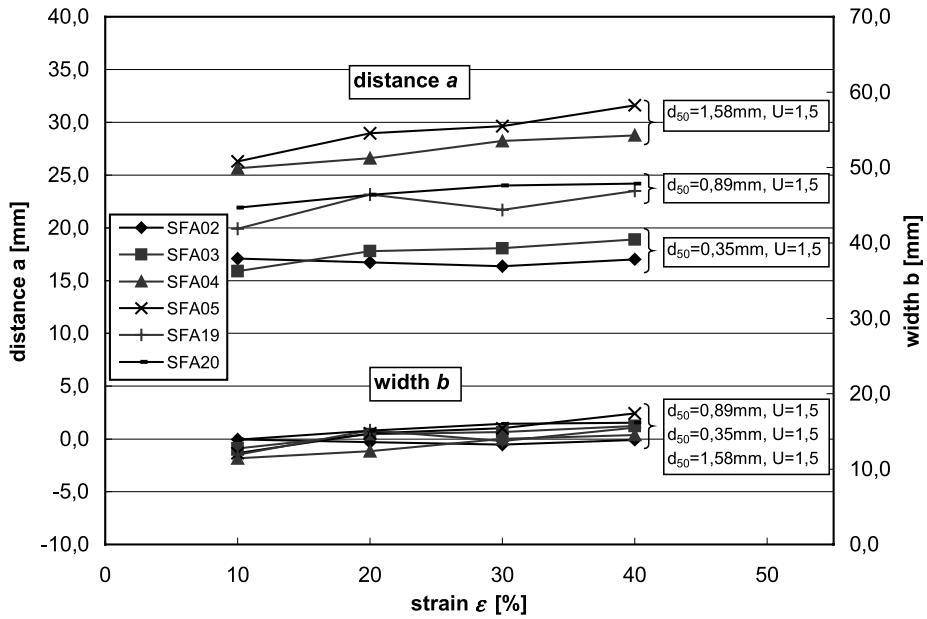

Fig. 10. Shear band distance a and width of the block b versus strain ϵ, variation of d_{50}.

principle stress directions. This leads to a change in the orientation of the principle stress direction and thus to the situation that one of the potential slip lines lies closer to a plane of maximum shearing rate and can therefore develop.

The thickness d_{SB} of the shear bands in the initial state varies between 6 and 13 times the average grain diameter and hence is in good agreement with the known theoretical and experimental investigations (Mühlhaus and Vardoulakis, 1987; Yoshida 1994; Oda and Kazama, 1998).

In Section 3.3.1 we pointed out that the results presented in

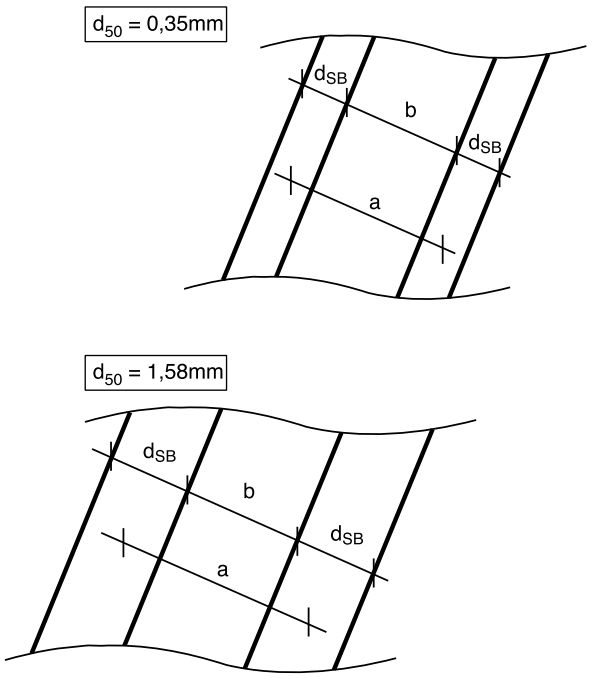

Fig. 11. Schematic change of thickness d_{SB}, width b, and distance a in relation to the influence of the granulometric parameters.

Fig. 6 might lead to the conclusion that the shear band distance a increases with increasing average grain size d_{50} and thus the shape of the shear band systems is dependent on this material parameter. If we take a look at the curves in Fig. 10, it is evident that the width b of the blocks between two adjacent shear zones hardly changes if sands with different average grain sizes d_{50} are investigated. Therefore the change in d_{50} is scarcely mirrored in a change of the width b but only in the well-known change in the shear band thickness d_{SB} (Fig. 11).

In contrast to the influence of the granulometric parameters, the observation of the width b of the blocks between the shear bands with respect to different initial heights of the specimen leads to the conclusion that, in addition to the distance a, b is also linearly dependent on the height of the sample and thus the height governs directly the shear band spacing. The thickness of the shear bands is constant for any experiment at a given stage of stretching due to the use of the same material for every test.

A very interesting point is the appearance of conjugate shear band systems in tests with coarse material and with a highly non-uniform sand (Fig. 12). Whereas the sand with higher non-uniformity produces only a few less distinctive conjugate shear bands, the ones in coarse sand are clear and make the same angle to either side of the vertical.

Referring to the influence of the dynamic material parameters, Poliakov's assumption that the shear band spacing changes with the variation of the factor B can be disputed. It is obvious that, in spite of the changing of the loading velocity and thus the changing of B from $B = 9$ to $B = 900$, the distances between the localisation zones are constant for the different tests at the same stage of stretching (Fig. 8). From their numerical simulations, Poliakov et al. (1994) expected that changes in B of the same magnitude result in definite variations of the shear band spacing a.

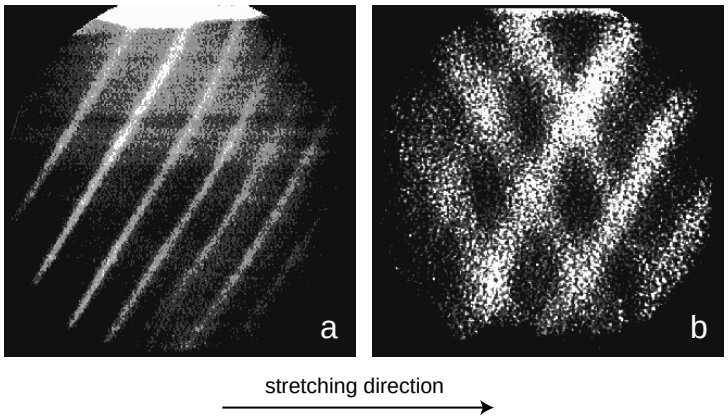

Fig. 12. Difference in grain shape depending on the average grain size d_{50}: (a) $d_{50} = 0.35$ mm and (b) $d_{50} = 1.58$ mm (material: quartz sand).

Furthermore the results show that the shape of the shear band systems is independent of the rate of loading.

According to Poliakov et al. (1994), changing the dynamic parameters while keeping B constant should not lead to changes in the shape of the developing shear band systems. As one can see in Fig. 9, this statement cannot be justified by our experiments. Although the material parameters of glass pearls and quartz sand coincide well (cf. Table 1), the results in Fig. 9 display differences in distance a as well as in inclination θ. We have to add, that this conclusion was drawn from a very 'general' reflection of the factor B and its properties. The results in Fig. 9 lead to the conclusion that additional material parameters, which are not reflected in Table 1, probably govern the spacing and the inclinations of the shear bands. Taking into account the observation of the experiments, it seems that the results are strongly influenced by the shapes and the surface properties of grains. We can justify this assumption by comparing again the results of experiments with glass pearls and fine sand as displayed in Fig. 9. Although the material parameters ($\gamma, d_{50}, U, G_{dyn}, \nu_p$) coincide very well, we observe different results with respect to the distances and the inclinations of the shear bands. In the quartz sand, grains are angular and rough; whereas glass beads are round and very smooth. Differences in the shear behaviour of granular material subject to the shape of the grains are documented in the literature (Dano, 2001; Schellart, 2000).

5. Conclusions

We may summarize our conclusions as follows:

1. The localisation of deformation develops spontaneously with uniformly distributed shear bands over the entire length of the specimen at amounts of strain between 2 and 6%. The failure zones remain active and planar during the entire process of straining. Additional shear zones do not develop, not even at high amounts of strain (up to 40%).
2. Supplementary strain after the localisation is accumulated predominantly in the existing failure zones. Just a small part of the imposed strain is gathered in the blocks between the shear bands.
3. In all experiments the inclination of the shear zones decreases with increasing strain while the distance between shear bands remains almost constant throughout the tests. The blocks rotate towards the moving wall.
4. The average grain size diameter d_{50} hardly influences the spacing between the localisation zones. In a granular material with a high coefficient of uniformity the mechanical behaviour and the material parameters related to the maximum grain size govern the shape of the developing shear bands.
5. The spacing of the shear zones is linearly dependent on the initial height of the specimens.
6. The shape of the shear band system is independent of the rate of loading.
7. The strong dependency of the shear band pattern on dynamic material parameters as proposed by Poliakov et al. (1994) in the form of the dimensionless parameter B has not been confirmed by our experimental investigations.

Acknowledgements

This work was supported by the Collaborative Research Center 526 "Rheology of the Earth" of the German Research Council (Deutsche Forschungsgemeinschaft, DFG). We thank Richard Norris, Jacques Desrues and Peter R. Cobbold for their constructive reviews of the manuscript. We thank Daniele Gualco, Dipartimento di Ingegneria Strutturale e Geotecnica, Università di Genova, for the evaluation of the experimental results in the framework of his diploma thesis.

References

Alshibli, A., Sture, S., 2000. Shear band formation in plane strain experiments on sand. Journal of Geotechnical and Geoenvironmental Engineering 126 (6), 495–503.

Arthur, J.R.F., Dunstan, T., 1982. Rupture layers in granular media. In: Vermeer, P.A., Luger, H.J. (Eds.), Proceedings of the IUTAM Symposium. Deformation and Failure of Granular Materials, Delft, pp. 453–459.

Arthur, J.R.F., Dunstan, T., Al-Ani, Q.A.J., Assadi, A., 1977. Plastic deformation and failure of granular media. Géotechnique 27, 53–74.

Bransby, P.L., Milligan, G.W.E., 1975. Soil deformation near cantilever sheet pile walls. Géotechnique 25, 175–195.

Brun, J.-P., Sokoutis, D., van den Driessche, J., 1994. Analogue modeling of detachment fault systems and core complexes. Geology 22, 319–322.

Cobbold, P.R., Durand, S., Mourgues, R., 2001. Sandbox modeling of thrust wedges with fluid-assisted detachments. Tectonophysics 334, 245–258.

Coulomb, C.A., 1773. Sur l'application des règles des maximis et minimis à quèlques problèmes de statique relatifs à l'architecture. Mémoires de Mathématique et de Physique, Académie Royale des Sciences 7, 343–382.

Dano, C., 2001. Comportement mecanique des sols injectes. Thèse de Doctorat. École centrale de Nantes.

Desrues, J., 1984. La localisation de la déformation dans les matériaux granulaires. PhD dissertation, Institut National Polytechnique de Grenoble, Grenoble, 283 pp.

Desrues, J., Lanier, J., Stutz, P., 1985. Localization of the deformation in tests on sand sample. Engineering Fracture Mechanics 21 (4), 909–921.

Desrues, J., Chambon, R., Mokni, M., Mazerolle, F., 1996. Void ratio evolution inside shear bands in triaxial sand specimens studied by computed tomography. Géotechnique 46 (3), 529–546.

Duthilleul, B., 1982. Rupture progressive: simulation physique et numérique. PhD dissertation, Institut National Polytechnique de Grenoble, pp. 1–260.

Finno, R.J., Harris, W.W., Mooney, M.A., Viggiani, G., 1997. Shear bands in plane strain compression of loose sand. Géotechnique 47, 149–165.

Gapais, D., Fiquet, G., Cobbold, P.R., 1991. Slip system domains. 3. New insights in fault kinematics from plane-strain sandbox experiments. Tectonophysics 188, 143–157.

Han, C., Drescher, A., 1993. Shear bands in biaxial test on dry coarse sand. Soils and Foundations 33 (1), 118–132.

Harper, T., Fossen, H., Hesthammer, J., 2001. Influence of uniform basement extension on faulting in cover sediments. Journal of Structural Geology 23, 593–600.

Ishikawa, M., Otsuki, K., 1995. Effects of strain gradients on asymmetry of experimental normal fault systems. Journal of Structural Geology 17 (7), 1047–1053.

Krantz, R.W., 1991. Measurement of friction coefficients and cohesion for faulting and fault reactivation in laboratory models using sand and sand mixtures. Tectonophysics 188, 203–207.

Lesnièwska, D., Mróz, Z., 2000. Limit equilibrium approach to study the evolution of shear band systems in soils. Géotechnique 50 (5), 521–536.

Lesnièwska, D., Mróz, Z., 2001. Study of evolution of shear band systems in sand retained by flexible wall. International Journal of Numerical Methods in Geomechanics 25, 909–932.

McClay, K.R., 1989. Analogue models of inversion tectonics. In: Cooper, M.A., Williams, G.D. (Eds.), Inversion Tectonics, Geological Society of London, Special Publication 44, pp. 41–59.

McClay, K.R., 1990. Deformation mechanics in analogue models of extensional fault systems. In: Knipe, R.J., Rutter, E.H. (Eds.), Deformation Mechanisms, Rheology and Tectonics, Geological Society of London, Special Publication 54, pp. 445–453.

McClay, K.R., Ellis, P.G., 1987a. Geometries of extensional fault systems developed in model experiments. Geology 15, 341–344.

McClay, K.R., Ellis, P.G., 1987b. Analogue models of extensional fault geometries. In: Coward, M.P., Dewey, J.F., Hancock, P.L. (Eds.), Continental Extensional Tectonics, Geological Society of London, Special Publication 28, pp. 109–125.

Mandl, G., 1988. Mechanics of Tectonic Faulting, Elsevier Science Publishers, Amsterdam.

Mandl, G., 2000. Faulting in Brittle Rocks, Springer-Verlag, Berlin–Heidelberg–New York.

Mandl, G., de Jong, L.N.J., Maltha, A., 1977. Shear zones in granular material. Rock Mechanics 9, 95–144.

Mokni, M., Desrues, J., 1998. Strain localization measurements in undrained plane-strain biaxial test on Hostun RF sand. Mechanics of Cohesive-Frictional Materials 4, 419–441.

Mühlhaus, H.-B., Aifantis, E.G., 1989. Strain localization in viscoplastic materials with microstructure. In: Dembicki, E., Gudehus, G., Sikora, Z. (Eds.), Proceedings of the 2nd International Workshop on Numerical Methods for Localization and Bifurcation of Granular Bodies, Gdansk, pp. 105–116.

Mühlhaus, H.-B., Vardoulakis, I., 1987. The thickness of shear bands in granular materials. Géotechnique 37, 271–283.

Nübel, K., Karcher, C., 1999. FE simulations of granular material with a given frequency distribution of voids as initial condition. Granular Matter 1, 105–112.

Oda, M., Kazama, H., 1998. Microstructure of shear bands and its relation to the mechanisms of dilatancy and failure of dense granular soils. Géotechnique 48, 465–481.

Papamichos, E., Vardoulakis, I., 1995. Shear band formation in sand according to non-coaxial plasticity model. Géotechnique 45 (4), 649–667.

Poliakov, A.B., Herrmann, H.J., Podladchikov, Y.Y., Roux, S., 1994. Fractal plastic shear bands. Fractals 2, 567–581.

Roscoe, K.H., 1970. The influence of strains in soil mechanics, 10th Rankine Lecture. Géotechnique 20, 129–170.

Saada, A.S., Liang, L., Figueroa, J.L., Cope, C.T., 1999. Bifurcation and shear band propagation in sands. Géotechnique 49 (3), 367–385.

Schellart, W.P., 2000. Shear test results for cohesion and friction coefficients for different granular materials: scaling implications for their usage in analogue modelling. Tectonophysics 324, 1–16.

Tatsuoka, F., Nakamura, S., Huang, C.-C., Tani, K., 1990. Strength anisotropy and shear band direction in plane strain tests of sand. Soils and Foundations 30 (1), 35–54.

Tejchman, J., Wu, W., 1993. Numerical study on patterning of shear bands in a Cosserat continuum. Acta Mechanica 99, 61–74.

Vardoulakis, I., 1980. Shear band inclination and shear modulus of sand in biaxial tests. International Journal for Numerical and Analytical Methods in Geomechanics 4, 103–119.

Vardoulakis, I., Goldscheider, M., 1980. Biaxialgerät zur Untersuchung der Festigkeit und Dilatanz von Scherfugen in Böden. Geotechnik 3, 19–31.

Vendeville, B., Cobbold, P.R., 1988. How normal faulting and sedimentation interact to produce listric fault profiles and stratigraphic wedges. Journal of Structural Geology 10 (7), 649–659.

Vendeville, B., Cobbold, P.R., Davy, P., Brun, J.P., Choukroune, P., 1987. Physical models of extensional tectonics at various scales. In: Coward, M.P., Dewey, J.F., Hancock, P.L. (Eds.), Continental Extensional Tectonics, Geological Society of London, Special Publication 28, pp. 95–107.

Vermeer, P.A., 1990. The orientation of shear bands in biaxial tests. Géotechnique 4, 3–119.

Viggiani, G., Kuentz, M., Desrues, J., 2001. An experimental investigation of the relationships between grain size distribution and shear banding in sand. In: Vermeer, P.A., Diebels, S., Ehlers, W., Herrmann, H.J., Luding, S., Ramm, E. (Eds.), Continuous and Discontinuous Modelling of Cohesive-Frictional Material, Springer, Stuttgart, pp. 111–126.

Wernicke, B., Burchfiel, B.C., 1982. Modes of extensional tectonics. Journal of Structural Geology 4 (2), 105–115.

Wichtmann, T., Sonntag, Th., Triantafyllidis, Th., 2001. Über das Erinnerungsvermögen von Sand unter zyklischer Belastung. Bautechnik 78 (12), 852–865.

Yoshida, T., 1994. Strain localization and shear banding during failure of sands. PhD Thesis, University of Tokyo.

Yoshida, T., Tatsuoka, F., 1997. Deformation property of shear band in sand subjected to plane strain compression and its relation to particle characteristics. Proceedings of the 14th International Conference of Soil Mechanics and Foundation Engineering, Hamburg, pp. 237–240.